J Mater Sci: Mater Med (2010) 21:2413–2423
DOI 10.1007/s10856-010-4093-6

An in vitro and in vivo investigation of the biological behavior of a ferrimagnetic cement for highly focalized thermotherapy

Ana Portela · Mário Vasconcelos · Rogério Branco · Fátima Gartner · Miguel Faria · José Cavalheiro

Received: 9 November 2008 / Accepted: 5 May 2010 / Published online: 15 June 2010

Abstract The cancer treatment by local hyperthermia, using a high frequency electromagnetic field is an extensively studied subject. For this propose it was developed a ferrimagnetic cement (FC) to be injected directly into the tumor. In this study it was determined the FC injectability, its capability to generate heat when placed within a magnetic field and its interaction with a modified simulated body fluid using SEM/EDS and XRD. The FC biological response was assessed by the intramuscular implantation in rats and histological analysis of the surrounding tissues. The results suggest that FC can be injected directly into the tumor, its temperature can be increased when exposed to a magnetic field and the surface of the immersed samples quickly becomes coated with precipitate denoting its ionic change with the surrounding medium. The histological analysis revealed a transient local inflammatory reaction, similar to the control material, only slightly more abundant during the first weeks, with a gradual decrease over the implantation time. Based on these results, we concluded that FC might be useful for highly focalized thermotherapy, with a good potential for clinical use.

A. Portela (✉) · M. Vasconcelos · R. Branco
Faculty of Dental Medicine, University of Porto, Porto, Portugal
e-mail: a.isabelportela@gmail.com

F. Gartner
IPATIMUP, University of Porto, Porto, Portugal

F. Gartner · M. Faria
ICBAS, University of Porto, Porto, Portugal

J. Cavalheiro
INEB/Engineering Faculty, University of Porto, Porto, Portugal

1 Introduction

The use of hyperthermia in oncology has been widely studied in recent decades. This kind of cancer treatment consists in the exposition of the affected tissues to temperatures that can vary between 42 and 47°C, what is achieved using different energy sources [1–3].

Current research focuses on its efficiency on several fronts. These include neovascularization of a neoplasm, with biological effects such as a decrease in the environmental pH and hypoxia of the neoplasm tissues, alteration of the biochemical mechanisms that regulate the cellular absorption of certain drugs and the triggering of immunological and apoptosis phenomena [4–8]. Some studies have reported that the localized heating of a solid tumor may apparently cause, in the long run, the destruction of the metastases of the neoplasm [6–8]. The methods currently available to produce hyperthermia are generally limited by the inability to selectively target the neoplasm cells, with the subsequent risk of affecting adjacent healthy tissues. If these tissues are also attacked, the induction of a selective immune response may be hindered [9, 10].

In a previous study (Almeida, Cavalheiro et al.), it was assessed a new method of neoplasm treatment by hyperthermia, the Highly Focalized Thermotherapy (HFT). This method consist in the direct injection of a material into the tumor and the subsequent exposition to an external high frequency magnetic field that will heat the magnetic particles and subsequently, the neoplasm cells [11]. For this purpose, Cavalheiro et al. [12] developed a material in the form of an injectable paste. Successful in vitro studies were performed to assess the biocompatibility of this material, which was later used in vivo to treat solid tumors. Treatments were effective in small tumors, with a significant

reduction of the tumor, but the injection of larger quantities in larger tumors was lethal to some animals, because of the material toxicity.

In an attempt to overcome this problem, the same author developed a new material to be used in the treatment of tumors using the previously described methodology. The composition of this new material, the ferrimagnetic cement (FC), is similar to the silicon–calcium cements but with a large amount of ferrimagnetic oxide. Over the past few years, many in vitro and in vivo experiments have been performed to establish the bioactivity of bioceramic materials, such as calcium phosphate, bioglass, and the silicon–calcium cements (the mineral trioxide aggregate, the Portland-like cements). These materials are indicated to use in orthopedics and in dentistry due to their osteoconductivity and bone replacement capability [13–15]. The main aim of this study was to assess if FC has suitable properties to be used in the HFT, determining its injectability, its specific heat capacity and, since FC will remain in the organism throughout the treatment period, is necessary to know the biological behavior of FC determined by in vitro and in vivo studies.

2 Methods and materials

The material which is the subject of this study, a ferrimagnetic silicate cement (FC), is a fine powder system which has a chemical composition in weight percent, based on oxides, corresponding to $10SiO_2$, $2Al_2O_3$, $52Fe_2O_3$, 0.6MgO, 33CaO, (SO_3 + K_2O) R. At the maximum powder/water combination ratio (3:2), the paste obtained flows, enabling the product to be injected.

2.1 Injectability

The injectability of FC was assessed by the ejection of the paste through disposable syringes, following a method that was adapted from the method described in the literature [16–18]. The injectable cement paste percentage was defined as the percentage resulting from the difference between the volume of expelled paste and the volume of the paste that was initially in the syringe; thus, the injectability percentage was calculated using the following formula:

$$\text{Injectable } \% = \text{Volume of paste ejected from the syringe} / \text{Total volume of paste before ejection}$$

2.2 Specific heating power

After mixing the FC samples with water, small discs of the solid material were placed in an isolated polyethylene tube with distilled water and exposed to a magnetic field (10 kHz) in a vertical coil (diameter 11 cm, 12 turns), using an induction system High Frequency Electronic Furnace K10/RV (CALAMARI and Milan, Italy). The variation of temperature was measured after 300 s of exposure to the magnetic field, using a digital thermometer. The specific heating power (P) was calculated according to the following formula:

$$P = \sum (Cp_i \cdot m_i) \cdot \Delta T/300,$$

where Cp_i and m_i are the specific heat capacity and the mass of each material (polyethylene, FC, water), respectively.

2.3 Characterization of the surface morphology and qualitative and semi-quantitative analysis

2.3.1 Scanning electron microscopy/energy dispersion spectroscopy (SEM/EDS)

The samples were prepared with the FC paste, in accordance with the pre-established powder/liquid ratio [19], which was placed in a 10 mm diameter and 5 mm high round mould, thus obtaining regular surfaces for later observation. After the material had set (98 min), the samples were removed from the mould. They were then divided into six groups, according to the different immersion times in a simulated physiological environment (SBF), after a preliminary study performed using the normal SBF medium during 4 days. The ion concentration of normal SBF, the synthetic plasma generally used in this kind of test, is similar to that of blood plasma [20]. In this study, after the preliminary evaluation using normal SBF, the calcium (Ca) that exists in natural plasma was replaced by strontium (Sr) to prepare the SBF Sr solution, thus enabling the identification of the source of the occasional precipitates that occur on the surface when the FC samples are immersed in this environment, without confusing the Ca of FC with that of the solution. Samples were immersed in SBF Sr at 37°C, for 1, 6, 10, 24, and 43 h, respectively. The control samples were not immersed. After the immersion period the samples were placed on carbon conductive tape in order to be observed and characterized using SEM and EDS. The surface of the FC sample, which is insulated, becomes conductive, due to the cathode deposit of a carbon film [21, 22].

The morphological analysis of the samples surface was performed using the SEM JEOL JSM-6301 (Joel Ltd, Japan) with an accelerating voltage of 15 kV and a working distance of 15 mm, at different magnifications (200×, 1000×, 2000×). It was also carried out an observation on retro-diffused electrons, locating the elements of high

atomic number (Sr, Fe) which, through this method, stand out in the image. Calcium, silicon, phosphorus, iron, magnesium, strontium, and carbon elements were accessed through qualitative and semi-quantitative microanalysis of the surface by EDS, using a Voyager system (Noran Instruments, Inc, USA).

2.3.2 X-ray diffraction

X-ray diffraction (XRD) analysis of FC samples control, prepared as described above, and FC samples immersed in SBF Sr for 7 days, was performed by a X'Pert Philips diffractometer, using CuK_1 radiation, Generator Settings: 50 mA, 40 kV with identification software PANalytical. The start position was (°2Th.) 3,5221 and the end position (°2Th.) 106,4421.

2.4 Measurement of the average size of the precipitates

Samples immersed for 10 and 24 h in SBF Sr were broken up to observe their cross-section, approximately perpendicular to the surface, viewing the crystals and enabling their measurement from the initial surface, to determine the average size of the precipitates formed. The variable studied is a continuous quantitative variable [23], and the average and standard deviations of each of the samples obtained were ascertained.

2.5 In vivo biocompatibility study

In order to assess the biocompatibility of FC, samples of this material and a control material were implanted in nine female Wistar rats (with an average weight of 200–230 g). During the trial period, the animals were treated in accordance with NP EN ISO 10993-2:2000 [24], taking in to account the animals welfare conditions and minimizing the number of laboratory animals used in tests. The animals were anesthetized with a combination of Ketamine (80–100 mg/kg) and Xylazine (5–10 mg/kg) by intraperitoneal injection [25].

The surgery consisted in the implantation of FC samples in the muscles on the left-hand side of the animal's flank, while the control, a low-density polyethylene (rounded samples with 4 mm diameter with a smooth surface) [26, 27], was implanted into the flank muscles on the right-hand side. Short-term tests were performed at 1, 3, and 9 weeks. Animals were euthanized using an overdose of intraperitoneal pentobarbital, and the implanted material was removed along with the adjacent tissues. The collected samples were immersed-fixed in 10% (v/v) formalin in 0.1 M phosphate buffer (pH = 7.4), embedded in paraffin, sectioned into slices of 5 μm thickness and then stained with haematoxylin and eosin. To assess the tissue response to the material, the fixed samples were observed under a LEICA Optical Microscope (LEICA DMLB, Q 500 IW) equipped with a photographic system that enables snapshots performed at microscopic observation of the samples. The biological response parameters were assessed and recorded according to ISO 10993-6:1994 [27], on the basis of:

(a) The extension of the fibrosis or fibrous capsule and inflammation response;
(b) The degeneration ascertained through alterations in the tissue morphology;
(c) The number and distribution, according to the distance between material/tissue, of types of inflammatory cells, namely polymorphic-nuclear leucocytes, lymphocytes, plasma cells, eosinophil, macrophages and multinucleate giant cells;
(d) The existence of necrosis, determined by the presence of nucleus remnants and/or capillary wall collapse;
(e) Other parameters, such as remnants of the material, fat infiltration and chronic granulomatous inflammation.

3 Results

3.1 Injectability

A correlation between the injectability and the setting time for the powder/water ratio used was previously determined according to ISO 9917:1:2003 [28]. When a higher powder/water proportion was used, the material, immediately after being mixed, revealed a significant increase in viscosity, preventing its injectability. Needle diameter also affects its injectability, since the cement does not flow through a diameter smaller than 1.6 mm.

For the determined powder/water combination ratio and with firm pressure, an injectability value corresponding to 90 ± 1% of the total FC paste volume was obtained, during the 5 min after the mixture.

3.2 Specific heating power

The system created to determine the FC specific heating power, exposed to a magnetic field, provides a maximum heating power of 2.11 W g^{-1}.

3.3 Characterization of the surface morphology and qualitative and semi-quantitative analysis

3.3.1 SEM/EDS

The results obtained through SEM and EDS of the FC surface samples were divided in five groups. Each group includes surface morphology images taken by SEM and

graphs illustrating the composition variation obtained using EDS analysis.

The initial cement surface of the control samples (Fig. 1) presents a very porous surface with macro (6–7 μm) and micro pores (2–3 μm). The calcium silicates and magnetite compounds (see XRD results) are detected in the EDS analysis where Fe, Ca and Si are dominant. In Fig. 2, relative to the samples surface immersed in normal SBF, it was observed a layer with precipitates of Ca and Mg phosphate compounds, with a decrease of Si and Fe.

After immersion for 1 h in SBF Sr (Fig. 3) a decrease in porosity can be observed, with the formation of precipitates over the initial surface. The spectrum analysis detected the presence of Sr and a decrease in Si. Samples immersed for 6 h (Fig. 4) have just small pores and an increasing formation of precipitates covering the surface. On EDS spectra of this layer we can observe the peaks of Ca, Mg, Sr, and also C. Over 43 h of immersion (Fig. 5) the initial FC surface is completely covered. The initial composition (manly Fe, Si) is not detected. The higher percentage of Sr results from the increased precipitation of the SBF Sr solution.

3.3.2 XRD

X-ray diffraction of FC control samples allow the identification of picks of the two major compounds of the cement: magnetite ($2\theta = 35.48$; 62.56), corresponding to d(Å) 2.530, 1.484 and calcium silicate Ca_3SiO_5 ($2\theta = 29.46$; 32.26; 34.40) corresponding to d(Å) 3.031, 2.775 and 2.607 respectively. After immersion in SBF Sr, the FC surface is covered with large crystalline precipitates of strontium carbonate. The main picks belong to $SrCO_3$ ($2\theta = 25.42$; 25.84; 36.64) corresponding respectively to d(Å) 3.503, 3.448 and 2.452. These results can be observed in Graph 1.

3.4 Measurement of the average size of the precipitates

Images taken after the FC samples broken up, displaying their cross-section, are presented in Fig. 6. The measurement of the average crystal size, in accordance with the corresponding scale displayed in the image, provided the results shown in Graph 2. The final average of the measurement of precipitates of the three surfaces immersed for 10 h in SBF Sr is 8.4 μm, corresponding to a development of 0.8 μm per hour. After 24 h of immersion, the precipitates have an average size of 24 μm, implying that there has been an average development of 15.6 μm (24–8.4 μm) over the 14 h period (10–24 h), corresponding to an average growing rate of 1.1 μm per hour. It was observed that the growth orientation of the precipitates occurs from the initial surface.

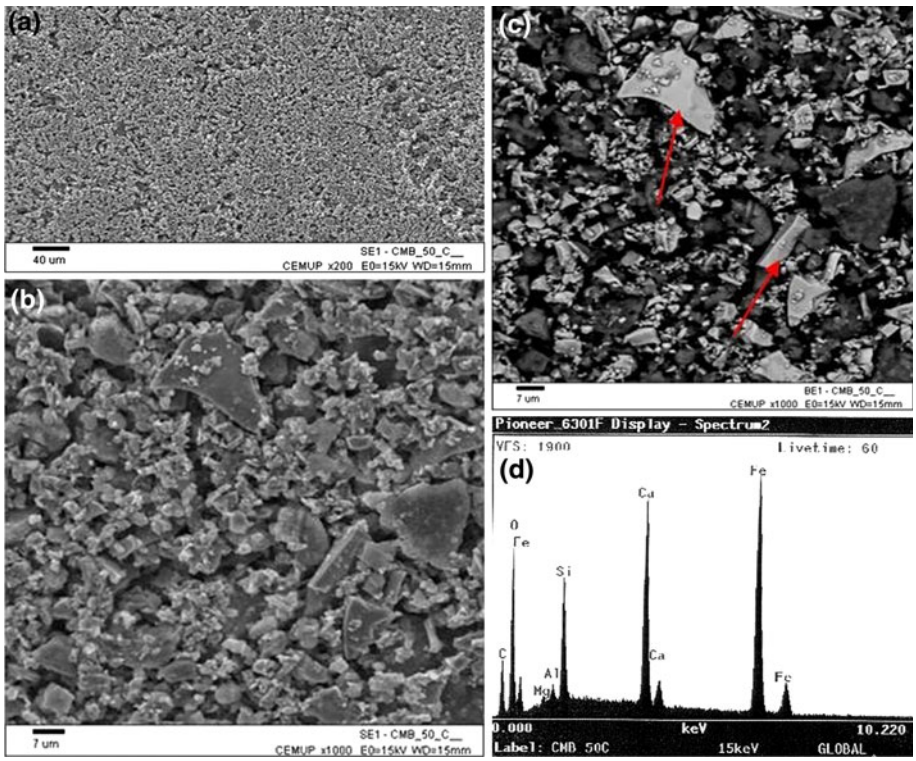

Fig. 1 FC control samples after cement preparation. **a** At ×200 magnification, a very porous surface. **b** The same image at a higher magnification (×1000). **c** In the retro-diffused electron image, shinier, lighter and larger particles corresponding to Fe, the high atomic number element (*arrows*). **d** Initial surface spectrum, where peaks of Fe, Ca and Si can be seen, as well as small percentages of Al and Mg, which are components of FC

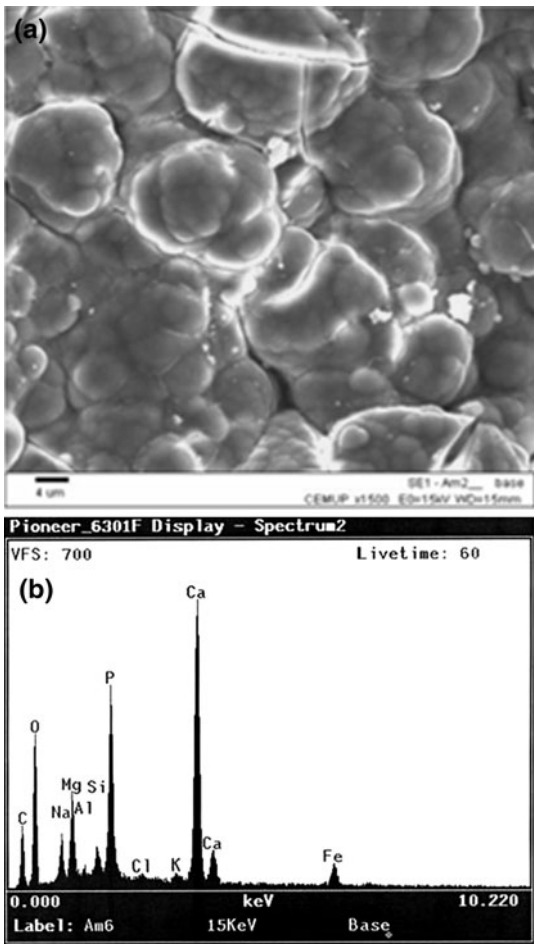

Fig. 2 FC samples immersed in normal SBF. **a** Precipitates covering the initial surface (×1500 magnification). **b** The precipitation of Ca and Mg phosphate compounds is detected. All the initial cement peaks of Si and Fe decreased and a high peak of P can be observed

3.5 In vivo biocompatibility study

The results obtained from histological observation 1 week after the implantation of the control material (Fig. 7a) and of FC samples (Fig. 8a) reveal an inflammatory infiltrate surrounding both materials, although the extent of this infiltrate and some of the cells that compose it are somewhat different.

The histological data regarding the samples obtained are compatible with a chronic inflammatory process in the control material samples and with a chronic foreign-body granulomatous inflammatory process in the FC samples.

Comparing the images correspondents to 3 and 9 weeks of the control material implantation (Fig. 7b, c) reveal that the layer of inflammatory cells surrounding the cystic lesion is thinner and has less inflammatory cells. The macrophages present in the images taken 3 weeks after the implantation are not visible in those taken after 9 weeks and the number of lymphocytes has significantly decreased.

FC samples also show a clear decrease in the inflammatory infiltrate throughout the implantation period (Fig. 8a, b, and c). Foreign-body reactive multinucleate giant cells were observed, in addition to other inflammatory cells. After 9 weeks the FC could be seen surrounded by muscle tissue with a thin layer of inflammatory cells.

4 Discussion

The use of an injectable self-setting biomaterial depends on its injectability properties, setting reaction, and setting time. However, there is no common procedure to measure injectability in relation to the setting time [29, 30]. The cement FC studied in this work is composed of several elements that make up the solid phase and uses water as the liquid phase, forming a paste when the two phases are mixed together.

The microstructure of this paste undergoes continuous transformation from the liquid phase to the solid phase. In this process the properties alteration of the cementing materials from viscous to viscous elastics the key to its injectability [30, 31]. The paste should be injected within a short working time, when viscosity is high. The determined FC powder/water ratio is easy to mix. The paste obtained enabled the injection of a substantial percentage of the sample (90 ± 1%), which can be handled within a reasonable period of time (5 min) and with an adequate setting time.

The treatment of tumors with hyperthermia, induced by magnetic materials and a magnetic field, has been developed by many researchers, with different approaches [32–37]. Since FC will be used in the treatment of solid tumors by this methodology, it's necessary that the FC has the capability to generate heat when exposed to a magnetic field. The in vitro evaluation of the specific heating power of FC, demonstrate a temperature increase in the FC sample environment (maximum heating power 2.11 W g^{-1}).

The comprehensive characterization of a material involves the study of a set of physical and chemical properties, as well as its microstructure. Detailed images were obtained using SEM and a rapid analysis of the chemical composition of small portions of the samples was made through EDS and XRD. In vitro studies involving the immersion of a material sample in a SBF are often used to assess bioactivity mechanisms, ascertaining the apparent biocompatibility of that material [20, 38]. The results observed in Fig. 2, after immersion during 4 days in normal SBF, show a surface completely covered with precipitates rich in calcium and phosphate allowing the conclusion that the FC exhibits a high bioactive behavior.

When examining the images of the FC surface characterized by SEM and EDS, before and after immersion in SBF Sr for 1, 6 and 43 h, respectively, significant

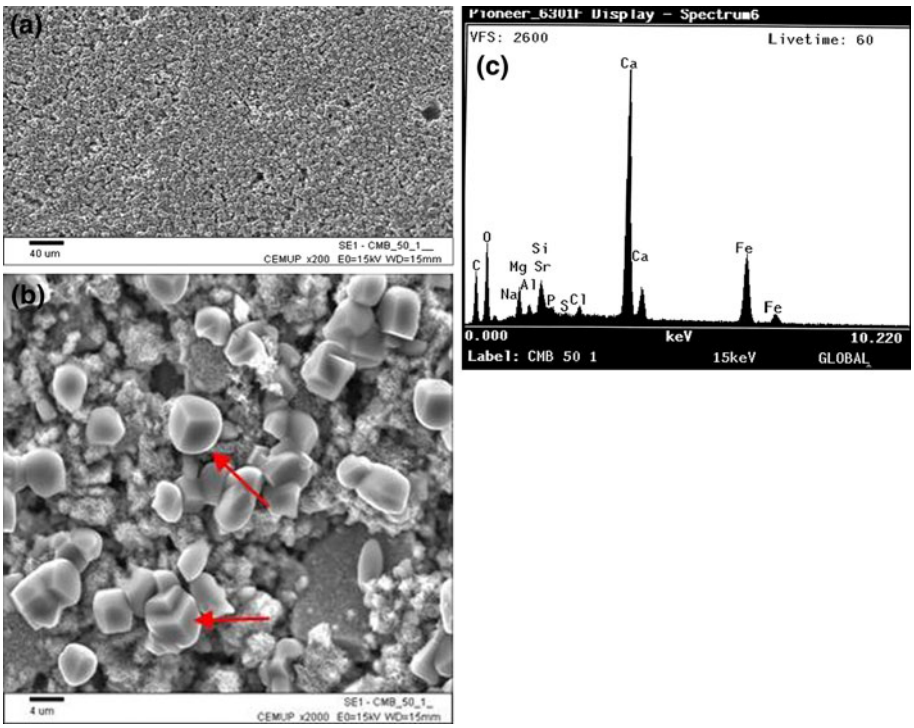

Fig. 3 FC samples immersed for 1 h in SBF Sr. **a** There is a general decrease in porosity, with 3–4 μm pores and smaller 1–2 μm pores observed at ×200 magnification. **b** A higher magnification (×2000) reveals, besides the pores, the formation of crystalline precipitates on the surface (*arrows*). **c** Surface spectrum displaying Ca, Fe and smaller percentages of Si, Mg, Al, and Cl, and the initial presence of Sr. The particles containing Fe and Si start to become covered with precipitates rich in Ca, and the Mg content increases

alterations were detected in the samples' morphology and composition over the immersion time. Along this period, the porous surface observed in the control samples was covered by a layer of precipitates and the final images (43 h immersion), revealed the continuous formation of precipitates emerging from those formed on the previous surface. The measurement of the average size of the crystals confirms the continuous formation of precipitates, with a progressive increase in the layer thickness, covering the whole original surface. The EDS analyses of the surface layer initially shows peaks of Ca, Si, Fe and Sr, the latter not present in the control samples of FC. On the surface the Si and Fe percentages decreased very quickly over the immersion time. The final surface layer is composed of Ca, Mg and Sr associated to high peaks of C and P which after crossing the EDS results with XRD analysis (Graph 1) prove to be mainly crystalline $SrCO_2$ in association with amorphous calcium compounds, because it was not possible to identify crystalline phases of phosphorus or carbonate calcium compounds. Due to the inexistence of Ca in the special SBF Sr medium, the existent Ca of the precipitate layer can only comes from the FC. Part of the cement will dissolve and the Ca will reprecipitate on the surface. Therefore, there was an ionic exchange between the initial cement sample and the surrounding environment. The physical structure of a material and the properties of its surface are known to be indicative of a material's biocompatibility [39]. The FC samples quickly become coated with precipitates, while the initial surface is covered with a layer resulting from interaction with the surrounding environment. These precipitates, when immersed in normal SBF, has an identical composition to that of the mineral constituents of bone. The changes in the compositions of the outer surface of FC, presuppose a biotolerated behavior in the organism, similar to other bioactive materials, such as calcium phosphate cements [40, 41], bioglasses [42, 43] and silicon–calcium cements [44, 45]. These materials share the capacity to interact with the surrounding environment and to form a layer on their surface that is essentially composed of carbonates and phosphates, among other elements present in their composition. Some authors report the formation of that layer on the surface of different materials during immersion in SBF and describe the bioactive behaviors as an ion exchange mechanism between the biomaterial and the physiological solution [46–49].

In vivo studies are essential for the assessment of medical devices, given that, their approval requires that they must be tested on animals before being used in humans [50]. Although in vitro studies provide information about certain elements (the cellular, molecular interaction with biomaterials), they cannot replace invivo studies, owing to the complexity of the biological medium [28, 51]. The success observed in the integration of biomaterial implants in tissues will depend on the capacity to mimic physiological responses, such as repair processes after lesion, and to control reactions such as inflammation [28, 52]. The mere act of implantation reveals the existence of tissue trauma which, in turn, induces a physiological scar formation process consisting of two basic components: inflammation and repair, which represent a vast interdependent network, where the

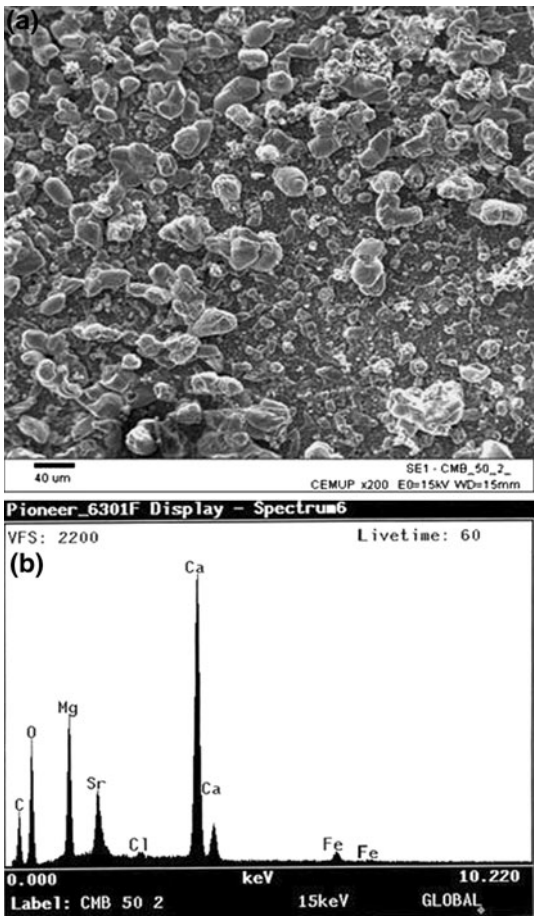

Fig. 4 FC samples immersed for 6 h in SBF Sr. **a** At ×200 magnification, only small pores are visible, along with the increasing formation of precipitates that cover the initial FC surface. **b** Spectrum of the surface composed of Ca, Mg, Sr and C, displaying the precipitates, which are coating it. The initial surface, marked by Fe, is almost totally covered

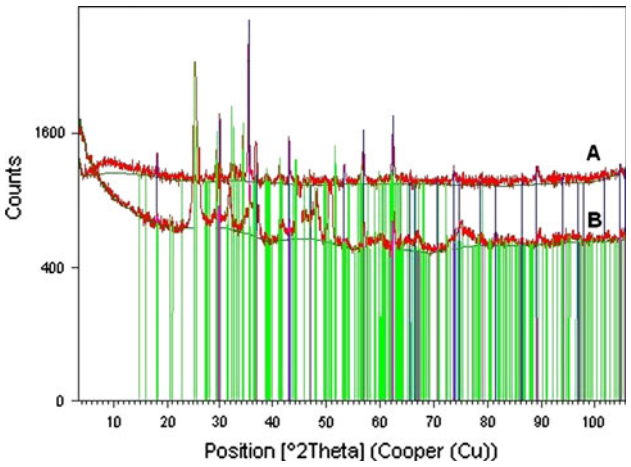

Graph 1 X-ray diffraction patterns of control samples **a** allow the identification of peaks of the two major compounds of the cement: magnetite ($2\theta = 35.48$; 62.56) and calcium silicate Ca_3SiO_5 ($2\theta = 29.46$; 32.26; 34.40), and **b** samples immersed 8 days in SBF Sr. The surface is covered with large crystalline precipitates. The main peaks belong to crystalline $SrCO_3$ ($2\theta = 25.42$; 25.84; 36.64)

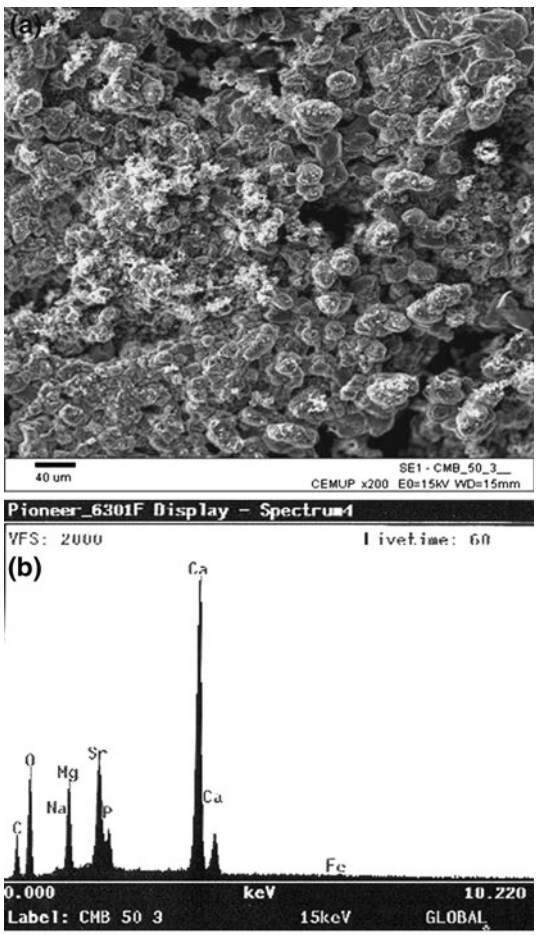

Fig. 5 FC samples immersed for 43 h in SBF Sr. **a** The initial FC surface is completely covered with precipitates, at ×200 magnification. **b** Spectrum of the sample surface that is covered with Ca, Sr, Mg, C, and P, resulting from interaction with the synthetic plasma

mediators of inflammation jointly act to trigger and control cellular response [53]. Assessment of the in vivo biocompatibility of FC was performed by its implantation in an animal model, which required a surgical procedure that causes lesions in the surrounding tissues.

Inflammation, the wound scarring process and the foreign-body responses of the organism are generally considered as the tissues' physiological response to lesions [54, 55]. The histological data regarding the samples obtained 1 week after implantation of the control material are compatible with a chronic inflammatory process mainly consisting of lymphocytes and macrophages, among other less relevant inflammatory cells surrounding the material. The physiological response of inflammation corresponds to a complex series of strictly controlled reactions, involving alterations in the expression of genes in blood cells (granulocytes, platelets, monocytes, lymphocytes), in inflammatory cells (macrophages, mastocytes) and in endothelial

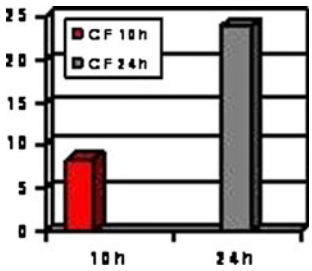

Graph 2 Measurement of the average size of the precipitates in the FC samples

cells, especially in the microcirculation of the tissues adjacent to the lesion. Although lymphocytes can be distinguished on the basis of their specific morphology, the different types of lymphocyte cells cannot be identified by conventional microscopy. Besides this, we cannot say much about their functional activity [55, 56]. However, the number of lymphocytes observed in this study is similar in both materials. Macrophages play a very important role in acute inflammation and probably in the biocompatibility of a material. They can release mediators that, in turn, activate other cells. It has been established that macrophages also affect the activity of fibroblasts and lymphocytes [57]. During the first week after the implantation of FC, a chronic foreign-body granulomatous inflammatory process was observed. Besides the inflammatory cells identified in the control material samples, a few foreign-body reactive multinucleate giant cells were found. The presence of foreign-body reactive multinucleate giant cells is important because it represents a specific inflammatory response triggered by the foreign substance [58]. The giant cells are present in small numbers and display their characteristic ring of particle remnants. Depending on the size of the implanted material's particles, the organism reacts in a different manner. Larger particles cannot undergo phagocytosis, thus remaining inside of the giant cells, producing a relatively inert tissue response [58, 59]. At the end of 3 weeks of implantation, a cystic lesion was observed around the control material, surrounded by a fine layer of inflammatory cells, mostly composed of lymphocytes and macrophages. The FC samples were very similar to those obtained after 1 week of implantation, only displaying a slight decrease in the inflammation around the cement, thus reducing the presence of inflammatory cells in the adjacent muscle tissue. The images of the implanted samples after 9 weeks display a significant decrease in the inflammatory response. In the control material, the cystic lesion surrounding it was coated with a fine layer of inflammatory cells, where only lymphocytes were detected. The FC samples revealed a fine layer of inflammatory cells, with lymphocytes and macrophages surrounding part of the cement. Owing to the absence of giant cells in these

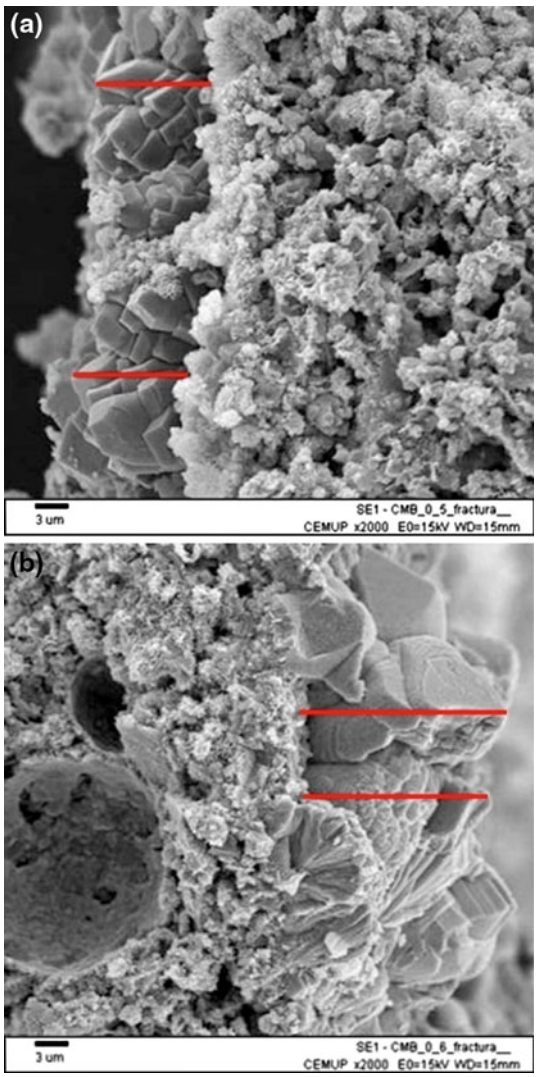

Fig. 6 **a** Broken up FC samples, after having been immersed for 10 h (×2000 magnification). **b** Broken up FC samples, after having been immersed for 24 h (×2000 magnification)

images, FC may be considered well tolerated. The most significant finding was the presence of cement in direct contact with the muscle tissue, displaying no inflammatory infiltrate. There was no necrosis in any of the samples, which is normally determined by the presence of nucleus remnants and/or capillary wall collapse, fat infiltration or granuloma. If a material is very toxic, it induces an acute local response for an indefinite period of time, but this did not occur with FC.

5 Conclusions

The FC object of this study will probably be considered a promising material to be utilized in the treatment of solid tumors with local hyperthermia. The fluid paste obtained can

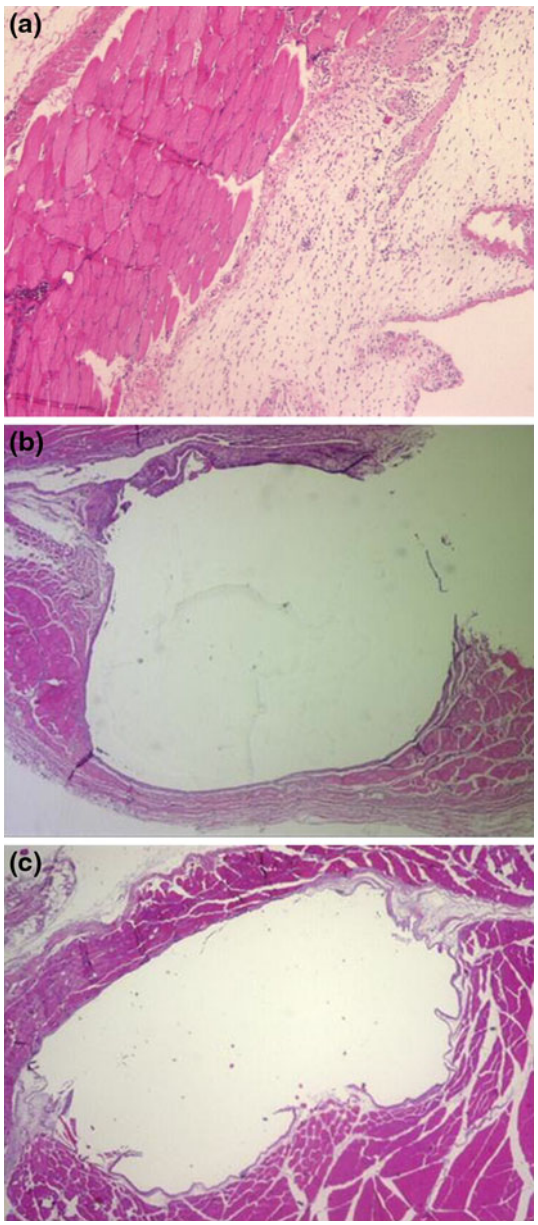

Fig. 7 Implantation of the control material (×50 magnification). **a** 1 week after intramuscular implantation of the control material. An inflammatory infiltrate is observed between the muscle tissue and the control material. The inflammatory cells are lymphocytes, macrophages and mastocytes, also present in the muscle tissue. **b** 3 weeks after implantation. These reveal an empty cystic lesion, corresponding to the control material implantation area and a thin layer of inflammatory cells limited to its peripheral area, without any significant infiltration of the adjacent muscle tissue. The inflammatory cells of the layer surrounding the cystic lesion are mostly lymphocytes and macrophages. **c** 9 weeks after implantation. These reveal that the cystic lesion that was observed at the end of 3 weeks of implantation still exists in the area of the control material. The presence of a few lymphocytes in the thin layer of inflammatory cells can be observed

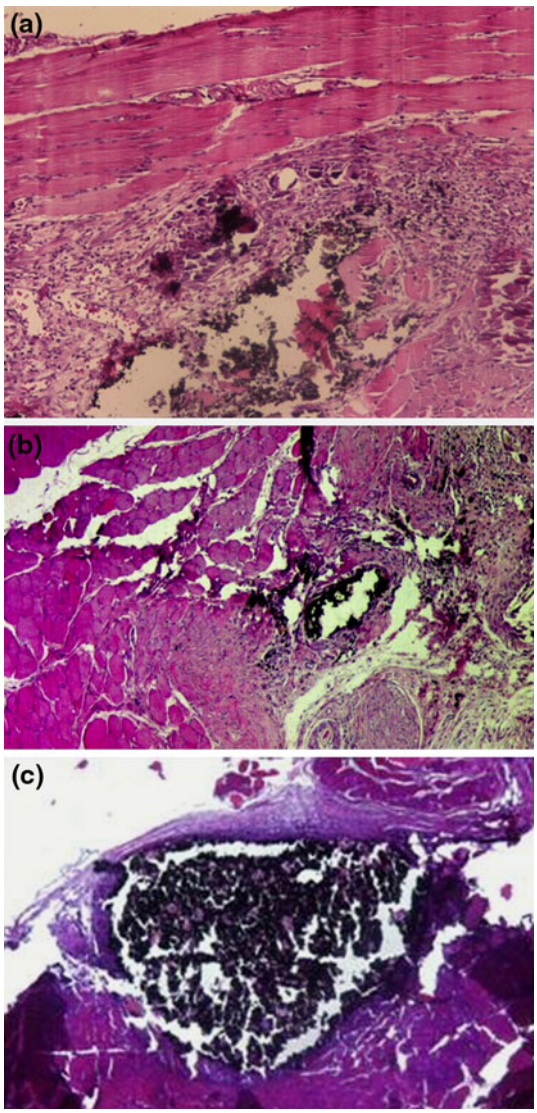

Fig. 8 Images of the intramuscular FC implantation area (×50 magnification). **a** After 1 week it is possible to see the nodular inflammatory lesion mainly composed of lymphocytes, some plasma cells, macrophages and multinucleate giant cells surrounding the FC (black-stained material). **b** 3 weeks after implantation. These display muscle tissue and, surrounding the cement, connective tissue and an inflammatory infiltrate. The inflammatory tissue that surrounds the cement is composed of a large amount of vascularized connective tissue and inflammatory infiltrate, mostly composed of macrophages, lymphocytes and foreign-body reactive multinucleate giant cells. **c** After 9 weeks. The FC is surrounded by muscle tissue in the lower portion of the sample and by an inflammatory infiltrate in the upper portion. The layer of inflammatory cells is clearly thinner than the layer observed after 3 weeks of implantation. Consequently, the number of inflammatory cells has also decreased, displaying only a few macrophages and lymphocytes

be directly injected into the solid tumors and it has the capability to generate heat when placed within a magnetic field.

In a normal or modified simulated body fluid immersion, FC surface's quickly becomes coated with a layer of precipitates that tends to stabilize. In the biological environment, the histological observation showed an

attenuation of the inflammatory infiltrate over the implantation time, denoting its biocompatibility. This data allows us to conclude that FC cement can remain in the inject site, the tumor, during a period of time enough to give repeated hyperthermia treatments using high frequency magnetic fields, providing a minimally invasive technique to treat solid tumors with HFT.

References

1. Lagendijk JJW. Hyperthermia treatment planning. Phys Med Biol. 2000;45:61–76.
2. Hildebrandt B, Wust P, Ahlers O. The cellular and molecular basis of hyperthermia. Crit Rev Oncol Hematol. 2002;43(1):33–56.
3. Van Der Zee J. Heating the patient: a promising approach? Ann Oncol. 2002;13(8):1173–84.
4. Alexander HR. Hyperthermia and its modern use in cancer treatment. Cancer. 2003;98(2):219–21.
5. Alexander HR. Cancer principles & practice of oncology. 7th ed. Philadelphia: Lippincott Williams and Wilkins; 2005. p. 2316–2821.
6. Shen R, Hornback NB, Shidnia H, Shupe RE, Brahmi Z. Whole-body hyperthermia decreases lung metastases in lung tumor-bearing mice, possibly via a mechanism involving natural killer cells. J Clin Immunol. 1987;7(3):246–53.
7. Dellian, et al. High-energy shock waves enhance hyperthermia response of tumors: effects on blood flow, energy metabolism, and tumor growth. J Natl Cancer Inst. 1994;86(4):287–93.
8. Rossi CR, Foletto M, Mocellin S, Pilati P, Lise M. Hyperthermia isolated limb perfusion with low-dose tumor necrosis factor-α and melphalan for bulky in-transit melanoma metastasis. Ann Surg Oncol. 2004;11(2):173–7.
9. Field SB. Physics and technology of hyperthermia. In: Field SB, Franconi C, editors. NATO ASI series, E: applied sciences. Dordrecht: Martinus Nijhoff Publisher; 1987. p. 19–27.
10. Szasz A. Hyperthermia, a modality in the wings. J Cancer Res Ther. 2007;3(1):56–66.
11. Almeida T. Estudo in vivo de um Cerâmico Ferrimagnético com potencial em Oncoterapia. Tese de Mestrado em Engenharia Biomédica pela Faculdade de Engenharia da Universidade do Porto. 2001.
12. Cavalheiro J, Vasconcelos M, Afonso A, Branco R. Ferrimagnetic and biocompatible cement for tumours thermotherapy. Bioceramics. 1996;9:243–6.
13. Xin R, Leng Y, Chen J, Zhang Q. A comparative study of calcium phosphate formation on bioceramics in vitro and in vivo. Biomaterials. 2005;26(33):6477–86.
14. Burguera EF, Xu HH, Takagi S, Chow LC. High early strength calcium phosphate bone cement: effects of dicalcium phosphate dihydrate and absorbable fibers. J Biomed Mater Res A. 2005; 75(4):966–75.
15. Islam I, Chng HK, Yap AU. X-ray diffraction analysis of mineral trioxide aggregate and Portland cement. Int Endod J. 2006;39(3): 220–5.
16. Khairoun I, Boltong MG, Driessens FCM, Planell JA. Some factors controlling the injectability of calcium phosphate bone cements. J Mater Sci. 1998;9(8):425–8.
17. Gou Z, Chang J, Zhai W, Wang J. Study on the self-setting property and the in vitro bioactivity of β-Ca_2SiO_4. J Biomed Mater Res B Appl Biomater. 2005;73(2):244–51.
18. Wang X, Ye J, Wang H. Effects of additives on the rheological properties and injectability of a calcium phosphate bone substitute material. J Biomed Mater Res B Appl Biomater. 2006; 78(2):259–64.
19. Portela A. Desenvolvimento de um novo cimento para termoterapia. Tese de Mestrado em Medicina Dentária Conservadora (Biomateriais) pela Faculdade de Medicina Dentária da Universidade do Porto. 2006.
20. Lu HH, Tang A, Oh SC, Spalazzi JP, Dionisio K. Compositional effects on the formation of a calcium phosphate layer and the response of osteoblast-like cells on polymer-bioactive glass composites. Biomaterials. 2005;26(32):6323–34.
21. Bentz DP, Stutzman PE. SEM analysis and computer modeling of hydration of Portland cement particles. Petrogr Cem Mat ASTM STP. 1994;1215:60–73.
22. Stuzman PE. Scanning electron microscopy in concrete petrography. Am Ceram Soc. 2000;1.
23. Dawson B, Trapp RG. Basic & clinical Biostatistics. 3rd ed. New York: McGraw-Hill; 2001. p. 28.
24. Wolfensohn S, Lloyd M. In: Wolfensohn S, editor. Handbook of laboratory animal management and welfare. Oxford: Blackwell Publishing; 2005. p. 233.
25. Norma Portuguesa. Avaliação biológica dos dispositivos médicos, Parte 2: Requisitos para o bem estar dos animais. NP EN ISO 10993-2. 2000.
26. Wolfensohn S, Lloyd M. In: Wolfensohn S, editor. Handbook of laboratory animal management and welfare. Oxford: Blackwell Publishing; 2005. p. 107.
27. Belanger MC, Marois Y. Hemocompatibility, biocompatibility, inflammatory and in vivo studies of primary reference materials low-density polyethylene and polydimethylsiloxane: a review. J Biomed Mater Res Appl Biomater. 2001;58(5):467–77.
28. International standard. Biological evaluation of medical devices—Part 6: Test for local effects after implantation. ISO 10993-6. 1994.
29. International organisation for standardization, dentistry-water-based cements—Part 1: Powder/liquid acid–base cements. ISO 9917-1. 2003.
30. Bohner M. Theoretical considerations on the injectability of calcium phosphate cements. In: Proceedings of the 17th European conference on biomaterials. Barcelona, Spain. 2002. p. 124.
31. Sarda S, Fernández E, Llorens J, Martínez S, Nilsson M, Planell JA. Rheological properties of an apatitic bone cements during initial setting. J Mater Sci Mater Med. 2001;12(10–12):905–9.
32. Moroz P, Jones SK, Gray BN. Magnetically mediated hyperthermia: current status and future directions. Int J Hyperth. 2002;18(4):267–84.
33. Suzuki M, Shinkai M, Honda H, Kobayashi T. Anticancer effect and immune induction by hyperthermia of malignant melanoma using magnetite cationic liposomes. Melanoma Res. 2003;13(2): 129–35.
34. Ito A, Tanaka K, Honda H, Abe S, Yamaguchi H, Kobayashi T. Complete regression of mouse mammary carcinoma with a size greater than 15 mm by frequent repeated hyperthermia using magnetic nanoparticles. J Biosci Bioeng. 2003;96(4):364–9.
35. Kawashita M, Tanaka M, Kokubo T, Inoue Y, Yao T, Hamada S, Shinjo T. Preparation of ferrimagnetic magnetite microspheres for in situ hyperthermic treatment of câncer. Biomaterials. 2005;26(15):2231–8.
36. Sato K, Watanabe Y, Horiuchi A, Yukumi S, Doi T, Yoshida M, Yamamoto Y, Tsunooka N, Kawachi K. Feasibility of new heating method of hepatic parenchyma using a sintered $MgFe_2O_4$ needle under an alternating magnetic field. J Surg Res. 2008;146:110–6.
37. Ito A, Saito H, Mitobe K, Minamiya Y, Takahashi N, Maruyama K, Motoyama S, Katayose Y, Ogawa J. Inhibition of heat shock

protein 90 sensitizes melanoma cells to thermosensitive ferromagnetic particle-mediated hyperthermia with low Curie temperature. Cancer Sci. 2009;100(3):558–64.
38. Oyane A, Kim HM, Furuya T, Kokubo T, Miyazaki T. Preparation and assessment of revised simulated body fluids. J Biomed Mater Res A. 2003;65(2):188–95.
39. Ratner BD, Hoffman A, Schoen FJ, Lemons JL. Biomaterials science: an introduction to materials in medicine. 2nd ed. London: Academic Press; 1996. p. 325–98.
40. Mirtchi AA, Lemaitre J, Munting E. Calcium phosphate cements: study of the β tricalcium phosphate dicalcium phosphate-calcite cements. Biomaterials. 1990;11:83–8.
41. Burguera EF, Xu HH, Takagi S, Chow LC. High early strength calcium phosphate bone cement: effects of dicalcium phosphate dihydrate and absorbable fibers. J Biomed Mater Res A 15. 2005;75(4):966–75.
42. Karlsson KH. Bioactivity of glass and bioactive glasses for bone repair. Eur J Glass Sci Technol A. 2004;45(4):157–61.
43. Thomas MV, Puleo DA, Al-Sabbagh M. Bioactive glass three decades on. J Long Term Eff Med Implants. 2005;15(6):585–97.
44. Zhao W, Wang J, Zhai W, Wang Z, Chang J. The self-setting properties and in vitro bioactivity of tricalcium silicate. Biomaterials. 2005;26:6113–21.
45. Zhao W, Chang J, Wang J, Zhai W, Wang Z. In vitro bioactivity of novel tricalcium silicate ceramics. J Mater Sci Mater Med. 2007;18:917–23.
46. Kokubo T, Miyaji F, Min-Kim H, Nakamura T. Spontaneous formation of bonelike apatite layer on chemically treated titanium metals. J Am Ceram Soc. 1996;79(4):1127–9.
47. Takadama H, Kim M, Kokubo T, Nakamura J. An X-ray photoelectron spectroscopy study of the process of apatite formation on bioactive titanium metal. J Biomed Mater Res. 2001;55(2):185–93.
48. Liang F, Zhou L, Wang K. Apatite formation on porous titanium by alkali and heat-treatment. Surf Coat Technol. 2003;165:133–9.
49. Spriano S, Bronzoni M, Verné E, Maina G, Bergo V, Windler M. Characterization of surface modified Ti–6Al–7Nb alloy. J Mater Sci Mater Med. 2005;16:301–12.
50. Stevens K. In vivo testing of biomaterials. BME. 2000;430(4):31–3.
51. Kirkpatrick CJ, Krump-Konvalinkova V, Unger RE, Bittinger F, Otto M, Peters K. Tissue response and biomaterial integration: the efficacy of in vitro methods. Biomol Eng. 2002;19:211–7.
52. Slavin J. The role of cytokines in wound healing. J Path. 1996;178(1):5–10.
53. Dee KC, Puleo DA, Bizios R. An introduction to tissue-biomaterial interactions. Tiss Biomater Int. 2003. doi:10.1002/0471270598.ch7.
54. Anderson JM. In vivo biocompatibility of implantable delivery systems and biomaterials. Eur J Pharm Biopharm. 1994;40:1–8.
55. Ryhanen J, Kallioinen M, Tuukkanen J, Junila J, Niemela E, Sandvik P, Serlo W. In vivo biocompatibility evaluation of nickel–titanium shape memory metal alloy: muscle and perineural tissue responses and encapsule membrane thickness. J Biomed Mater Res. 1998;41:481–8.
56. Kirkpatrick CJ, Otto M, Van Kooten T, Krump V, Kriegsmann J, Bittinger F. Endothelial cell cultures as a tool in biomaterial research. J Mater Sci Mater Med. 1999;10:589–94.
57. Anderson JM, Miller KM. Biomaterial, biocompatibility and the macrophages. Biomaterials. 1984;5:5–10.
58. Thomsen P, Ericson LE. Inflammatory cell response to bone implant surfaces. In: Davis JE, editor. The bone biomaterial interface. Toronto: University of Toronto Press. 1991. p. 153–164.
59. Hallam JBP. The interaction of biomaterials with the body is a two way phenomenon-long. Sci Today. 2002;20:420–3.